Journal of Mathematical Systems, Estimation, and Control
Vol. 8, No. 2, 1998, pp. 1–20

Spectral Element Approximations and Infinite Domains*

Kelly Black

Abstract

A spectral-element technique to approximate partial differential equations on an infinite domain is examined. The method is based on Boyd's mapping of a semi-infinite interval to a finite interval, and it is extended to a variational setting which allows for an implementation using a spectral-element method. By extending the method to a variational form, a straight-forward implementation allows for high order approximations over an infinite computational domain.

1 Introduction

Partial Differential Equations (PDEs) on either infinite or semi-infinite domains arise in many applications. For example, for a problem that includes an electromagnetic field in 3-D, the field may need to be extended to an infinite interval to simulate total absorbing boundary conditions. One of the difficulties in dealing with the infinite interval is that these fields decay to zero but only decay algebraically depending on the dimension [1, 9, 13, 15, 16]. The approximation of the resulting equations can give rise to many practical difficulties, especially when Laguerre or Hermite polynomials are employed to approximate the equations.

The approximation of PDEs on infinite domains has proceeded on various fronts. For high order methods, such as spectral elements, the most common method is through the use of polynomials which are orthogonal over a semi-infinite domain. Such methods suffer from a variety of drawbacks. For example, Laguerre polynomials scale quite badly for large polynomial degrees [4] and offer poor convergence for approximating solutions that do not decay to zero exponentially [2].

*Received November 5, 1996; received in final form June 26, 1997. Summary appeared in Volume 8, Number 2, 1998. This paper was presented at the Conference on Computation and Control V, Bozeman, Montana, August 1996. The paper was accepated for publication by special editors John Lund and Kenneth Bowers.

To avoid these difficulties, Boyd has proposed a method that proceeds by mapping a semi-infinite interval to a finite interval [2]. The method is commonly used for relatively simple geometries where a single computational domain can be employed. The method is adapted for use in the spectral element method. By adapting the method to allow for a variational approach, the spectral element method can be extended to allow for semi-infinite subdomains.

A numerical method is proposed in which the computational domain is divided into non-overlapping subdomains. The semi-infinite subdomains are approximated by first mapping them to finite subdomains through the use of an algebraic mapping [2]. An example is given for the approximation of the Helmholtz equation. Numerical examples are given for the method for the approximation of Navier Stokes incompressible flow as well as a comparison with Laguerre polynomial approximations.

2 Spectral Elements

Spectral elements are employed to build high-order approximations to avoid some of the restrictions of single domain spectral methods. The spectral element method allows for approximations on more complicated geometries when compared to a single domain spectral method by dividing the domain of a problem into non-overlapping subdomains. Within each subdomain, an approximation is constructed as a linear combination of high order orthogonal polynomials.

Specifically, Legendre polynomials are used to build a variational formulation. Such an approach is essentially the $h-p$ finite element method and allows for simple p-refinement. The traditional spectral element method builds on the collocation method, in which the approximation is found from the polynomial interpolating on the abscissa of the Gauss-Lobatto quadrature. Here an approximation is constructed in the spectral space. The approximation is found as a linear combination of the Legendre polynomials.

A simple test case is examined, to demonstrate the spectral element method with a local Fourier basis. The method is demonstrated for a simple Helmholtz equation, and an application to Navier-Stokes incompressible flow over a back-step is given. The method is then extended to a semi-infinite computational domain. This is done by first examining Laguerre polynomials, and finally a new method is given which is based on the work of Boyd [2]. In this method, the semi-infinite subdomains are mapped to a finite domain via an algebraic mapping. Once done, a variational form is derived.

2.1 Introduction to spectral elements with local spectral basis

An approximation is found in the spectral space. In order to find the approximation, the space of polynomials up to degree N is divided into the polynomials that are zero on the boundaries and those that are not,

$$\phi_i(x) = \begin{cases} \frac{1+x}{2} & i = 0, \\ \frac{1-x}{2} & i = 1, \\ L_i(x) - L_{i-2}(x) & i > 1, \end{cases} \tag{2.1}$$

for $i = 0 \ldots N$, and $L_i(x)$ is the i^{th} Legendre polynomial. The span of the test functions is the span of polynomials up to degree N, and each of the ϕ_i's are linearly independent. The choice of these functions is motivated by the results of Shen [14]. As will be seen, the resulting stiffness matrix for the 1D problem is nearly diagonal, and the mass matrix is tridiagonal. (Because the mass matrix is not diagonal inverting the relevant systems of equations leads to a greater number of operations.) Since a tensor product of the basis functions is used for the higher dimensional problems, the result is a very sparse system of equations. The primary difference from the work of Shen [14] is the addition of ϕ_0 and ϕ_1, and implementing it as a spectral element method. The two new linear basis functions are used to form a hat function whose support includes adjacent subdomains.

To present the method and to avoid too many technical details, a simple 1D Helmholtz equation is examined first,

$$\begin{aligned} u_{xx} + \lambda u &= f(x), \\ x &\in (-1, 1), \\ u(\pm 1) &= 0. \end{aligned} \tag{2.2}$$

If the domain, $(-1, 1)$, is divided into two subdomains, $(-1, 0)$ and $(0, 1)$ (see Figure 1), then within each subdomain, an approximation is constructed as a linear combination of the basis functions,

$$u_N^0(x) = \sum_{i=0}^{N} \hat{u}_i^0 \phi_i^0(x), \qquad x \in (-1, 0), \tag{2.3a}$$

$$u_N^1(x) = \sum_{i=0}^{N} \hat{u}_i^1 \phi_i^1(x), \qquad x \in (0, 1), \tag{2.3b}$$

where the basis functions are defined within each subdomain,

$$\phi_i^0(x) = \phi_i(2x + 1), \tag{2.4a}$$

$$\phi_i^1(x) = \phi_i(2x - 1). \tag{2.4b}$$

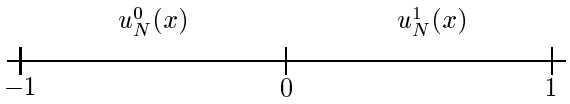

Figure 1: A Multi-Domain Example in 1-D for subdomains 0 and 1.

To build the linear system of equations to approximate equation (2.2), a variational form for each test function is constructed. First, on subdomain 1, the variational form for the test functions which are zero at the subdomain interfaces is found,

$$-\int_{-1}^{0} \left(u_N^0(x)\right)_x \left(\phi_m^0(x)\right)_x dx + \int_{-1}^{0} \lambda u_N^0(x)\phi_m^0(x)dx = \int_{-1}^{0} f_N(x)\phi_m^0(x)dx, \tag{2.5}$$

for $m = 2 \ldots N$. Next, the variational form for the test functions which are zero at the subdomain faces is found for subdomain 1,

$$-\int_{0}^{1} \left(u_N^1(x)\right)_x \left(\phi_m^1(x)\right)_x dx + \int_{0}^{1} \lambda u_N^1(x)\phi_m^1(x)dx = \int_{0}^{1} f_N(x)\phi_m^1(x)dx, \tag{2.6}$$

for $m = 2 \ldots N$. Next the variational form for the hat function spanning the two subdomains is constructed (see Figure 2),

$$\begin{aligned} &-\int_{-1}^{0} \left(u_N^0(x)\right)_x \left(\phi_0^0(x)\right)_x dx + \int_{-1}^{0} \lambda u_N^0(x)\phi_0^0(x)dx \\ &-\int_{0}^{1} \left(u_N^1(x)\right)_x \left(\phi_1^1(x)\right)_x dx + \int_{0}^{1} \lambda u_N^1(x)\phi_1^1(x)dx = \\ &\qquad \int_{-1}^{0} f_N(x)\phi_0^0(x)dx + \int_{0}^{1} f_N(x)\phi_1^1(x)dx. \end{aligned} \tag{2.7}$$

Finally, the boundary conditions are enforced, and continuity at the subdomain interface is enforced,

$$\begin{array}{lllllll} u_N^0(0) & = & \hat{u}_0^0 & = & u_N^1(0) & = & \hat{u}_1^1. \\ u_N^0(-1) & = & \hat{u}_1^0 & = & 0, & & \\ u_N^1(1) & = & \hat{u}_0^1 & = & 0. & & \end{array} \tag{2.8}$$

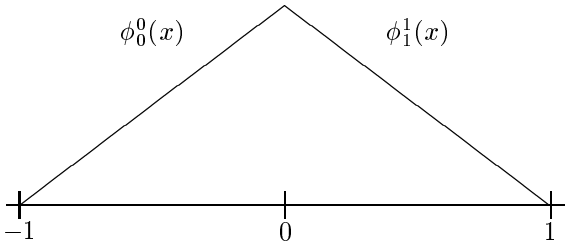

Figure 2: Trial functions $\phi_0^0(x)$ and $\phi_1^1(x)$ combine on adjacent subdomains to assemble a "hat" function on adjacent subdomains.

To build the linear system of equations, the approximations, equations (2.3a) and (2.3b), are substituted into the variational formulation given in equations (2.5) through (2.8). For example, the stiffness matrix, $\mathcal{S}_N$, can be found, by first substituting equation (2.3a) into the variational form,

$$-\int_{-1}^{0} \left(u_N^0(x)\right)_x \left(\phi_m^0(x)\right)_x dx \quad = \quad \sum_{i=0}^{N} \hat{u}_i^0 \left(-\int_{-1}^{0} \left(\phi_i^0(x)\right)_x \left(\phi_m^0(x)\right)_x dx \right) \tag{2.9}$$

The stiffness matrix can then be defined,

$$\left(\mathcal{S}_N\right)_{mi} \quad = \quad -2\int_{-1}^{1} \left(\phi_i(x)\right)_x \left(\phi_m(x)\right)_x dx. \tag{2.10}$$

In this Galerkin formulation, the choice of test functions, $\phi_i(x)$, offers an advantage. As pointed out by Shen [14],

$$\begin{aligned} -\int_{-1}^{1} \left(L_i(x) - L_{i-2}(x)\right)' \left(L_i(x) - L_{i-2}(x)\right)' dx \qquad & (2.11) \\ = -\int_{-1}^{1} \left(2i-1\right) L_{i-1}(x) \left(2j-1\right) L_{j-1}(x) dx, \\ = -\left(2i-1\right)\left(2j-1\right), \int_{-1}^{1} L_{i-1}(x) L_{j-1}(x) dx \\ = -2\left(2i-1\right)\delta_{ij}. \end{aligned}$$

The final result follows from the orthogonality of the Legendre polynomials. The result is that the stiffness matrix for the 1D problem is diagonal for rows greater than 1, and is block diagonal (2×2) on rows 0 and 1 (see Figure 3). The mass matrix is tridiagonal, and since a tensor product is used for higher dimensions, the result is a sparse linear system.

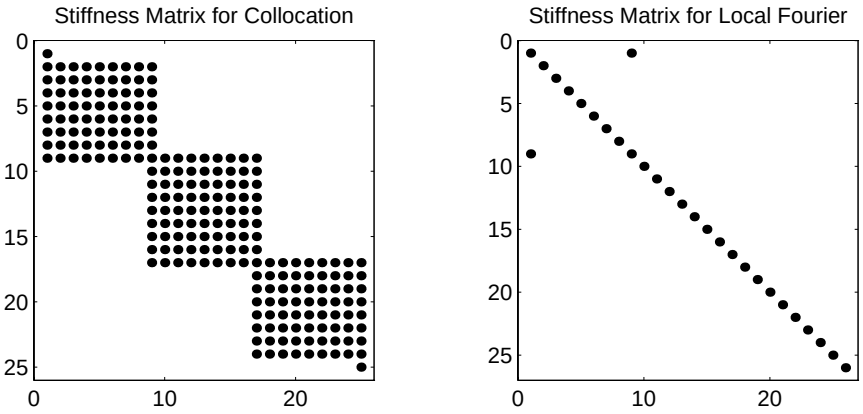

Figure 3: Comparison of the stiffness matrix for the collocation and the local spectral schemes.

2.2 Spectral element approximation of Navier-Stokes incompressible flow

As a demonstration of a 2D approximation, the incompressible Navier-Stokes flow equation,

$$\begin{aligned} \mathbf{u}_t + (\mathbf{u}\cdot\nabla)\mathbf{u} + \nabla p &= \frac{1}{\mathrm{Re}}\nabla^2\mathbf{u}, \\ \text{subject to } \nabla\cdot\mathbf{u} &= 0, \end{aligned} \tag{2.12}$$

with no slip boundaries is examined [6]. The geometry examined is for flow over a backstep. The spatial discretization employed is the same as examined in section 2. The temporal discretization is based on the the splitting method [10] and the methods proposed by Karniadakis, et al [8]. The splitting method is a convenient scheme to separate the actions of the two spatial operators acting on the velocity,

$$\begin{aligned} \mathcal{N}(\mathbf{u}) &= \frac{1}{2}\left((\mathbf{u}\cdot\nabla)\,\mathbf{u} + \nabla\cdot(\mathbf{u}\mathbf{u})\right), \\ \mathcal{L}(\mathbf{u}) &= \frac{1}{\mathrm{Re}}\nabla^2\mathbf{u}. \end{aligned} \tag{2.13}$$

(The implementation employs the skew-symmetric form of the nonlinear operator).

Following the method proposed by Karniadakis, et al [8], the pressure is not calculated, rather the time averaged pressure is approximated. The

three relevant spatial operators can then be isolated in three separate steps,

$$\tilde{\mathbf{u}}_N - \mathbf{u}_N^n = -\int_{t_n}^{t_{n+1}} \mathcal{N}(\mathbf{u}_N)\, dt, \tag{2.14a}$$

$$-\tilde{\mathbf{u}}_N + \hat{\mathbf{u}}_N = -\nabla \bar{p}, \quad \text{subject to } \nabla \cdot \hat{\mathbf{u}}_N = 0, \tag{2.14b}$$

$$\mathbf{u}_N^{n+1} - \hat{\mathbf{u}}_N = \int_{t_n}^{t_{n+1}} \mathcal{L}(\mathbf{u}_N)\, dt. \tag{2.14c}$$

In the first time step the nonlinear term is integrated through the use of an explicit method such as those from the Adams-Bashforth family of schemes while the third step employs an implicit step such as those found in the Adams-Moulton family of schemes. Because an explicit step is taken there is a restriction on the time step. However, the more stringent restriction on the time step comes from the Stokes operator. This is mitigated through the use of the implicit step in the final equation.

The boundary conditions are found in the same manner as that proposed by Karniadakis, et al [8], and Neumann type boundaries are employed [6]. For the pressure calculation, the boundaries are calculated by splitting the Laplace operator into its solenoidal and irrotational parts. Because the divergence of the velocity is to be zero at a future time step, an implicit scheme is used to integrate the irrotational part of the operator, while an explicit scheme is used for the solenoidal part.

For the 2D equations, both the basis and test functions are taken as tensor products of those found in the 1D case. Within each subdomain an approximation is constructed which is a linear combination of the Legendre polynomials, for (x, y) in subdomain r,

$$u_N^r(x, y) = \sum_{j=0}^{N} \sum_{i=0}^{N} \hat{u}_{ij}^r \phi_i^r(x) \phi_j^r(y). \tag{2.15}$$

The test functions are also found as a simple tensor product, $\phi_j^r(x)\phi_i^r(y)$.

Continuity across the subdomain interfaces are enforced by minimizing the difference between the approximations on adjacent subdomains. For example, if subdomain r is to the right of subdomain l then on subdomain r the boundary $x^r = -1$ is adjacent to the boundary on subdomain l when $x^l = 1$ (see Figure 4). The continuity across this interface is enforced by requiring that the difference between the two approximations be orthogonal to the space of polynomials of degree N,

$$\int_{-1}^{1} \left(u_N^l(1, y) - u_N^r(-1, y)\right) L_j(y) dy = 0, \qquad j = 0 \ldots N. \tag{2.16}$$

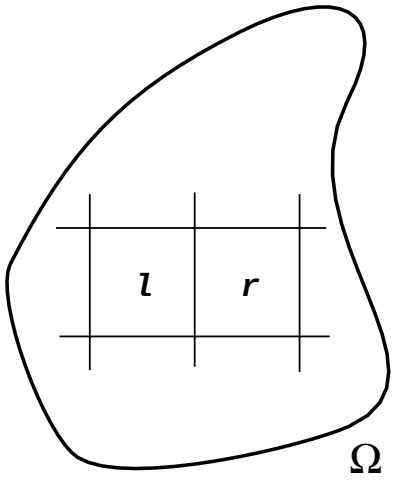

Figure 4: Example of two adjacent subdomains, subdomain l and r.

If a conforming method is employed, continuity is insured when $\hat{u}^l_{0i} = \hat{u}^r_{1i}$, for $i = 0 \ldots N$ since the basis functions are linearly independent.

An example of the results of such an approximation is shown in Figure 6. In the example, the velocity field is shown for two different Reynolds numbers, Re=200 and Re=400. Because the domain can be divided into separate subdomains (see Figure 5), a more complex geometry can be accommodated when compared to a single domain spectral method.

3 Laguerre Polynomials

At first glance, the Laguerre polynomials seem to be a natural candidate for approximating PDE's on a semi-infinite domain. The Laguerre polynomials, denoted $L^{(0)}_i(x)$ for the i^{th} Laguerre polynomial, are orthogonal on the semi-infinite domain with respect to the weight function e^{-x} [5],

$$\int_0^\infty L^{(0)}_i(x) L^{(0)}_j(x) e^{-x} dx \quad = \quad \delta_{ij}. \tag{3.1}$$

There is an abundance of theoretical results on Laguerre polynomials. Most noticeably, both Funaro [3] and Maday [11] have shown many theoretical results on the accuracy of such methods. However, in practice, there are also many difficulties associated with Laguerre polynomials [12]. First,

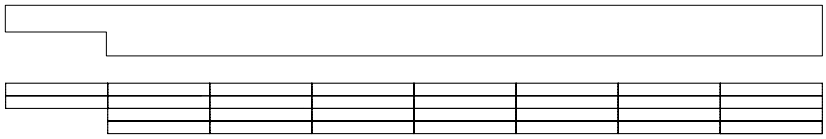

Figure 5: Flow over a backstep and the domain decomposition.

the Laguerre polynomials scale quite badly for the larger degree polynomials [4]. Moreover, the Laguerre polynomials suffer considerably in the small range of boundaries that can be accommodated at infinity [12]. Finally, the Laguerre polynomials experience spectral convergence only for solutions that decay to zero exponentially [2].

On the positive side, for approximations to solutions that decay exponentially to zero, Laguerre polynomials offer a simple implementation. For example, for a spectral element method, semi-infinite domains can be accommodated through the following basis functions,

$$\phi_0(x) = L_0^{(0)}(x)e^{-x/2}, \tag{3.2a}$$

$$\phi_i(x) = \left(L_i^{(0)}(x) - L_{i-1}^{(0)}(x)\right) e^{-x/2}, \quad i > 0. \tag{3.2b}$$

Through these basis elements a variational approximation can be constructed. This is made easier since, as defined, the basis functions satisfy the following identities,

$$\phi_0(0) = 1, \tag{3.3a}$$

$$\phi_i(0) = 0, \qquad i > 0, \tag{3.3b}$$

$$\frac{d}{dx}\left(L_i^{(0)}(x) - L_{i-1}^{(0)}(x)\right) = -L_{i-1}^{(0)}(x), \qquad i > 0. \tag{3.3c}$$

Here the function $\phi^0(x)$ is employed to form a basis function whose support includes two adjacent subdomains. The technique is used in the same manner as in the situation with finite subdomains, and the resulting stiffness and mass matrices are both symmetric and tridiagonal.

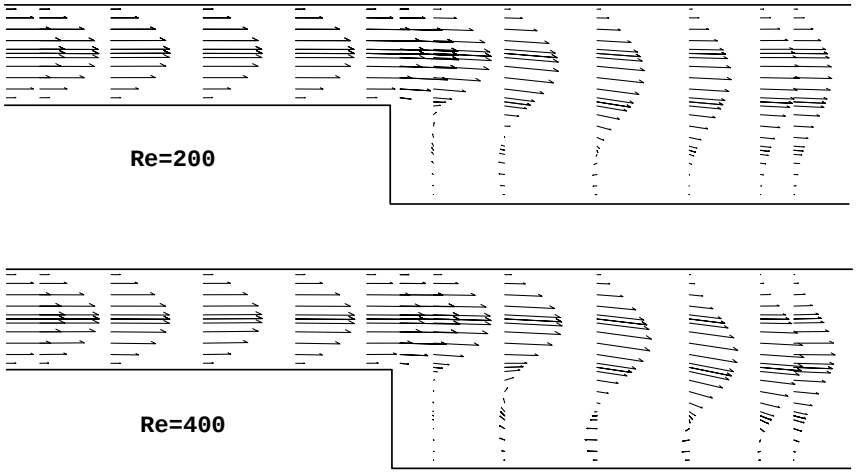

Figure 6: Spectral element approximation of flow past a back-step. The approximation within each subdomain consists of a polynomial of degree 6 in both the x and the y directions. The maximum velocity at the inlet is one and the height of the step is one half.

4 Algebraic Mapping

Another common method for building an approximation on a semi-infinite domain is through the use of the algebraic mapping proposed by Boyd [2]. By mapping the semi-infinite interval, $[0, \infty)$, to a finite interval, $[-1, 1]$. Orthogonal polynomials can be constructed to construct an approximation on the finite interval.

The method proposed is first introduced and a simple 1D example is given. Once done, comparisons are given between the mapping and Laguerre polynomials. In the examples, a 1D Helmholtz equation is examined on an infinite domain. In the first comparison, the solution to the equation decays to zero exponentially, while in the second example, the solution decays to zero algebraically.

4.1 Mapping to a finite subdomain

We propose to adapt the mapping first proposed by Boyd [2],

$$y = M\frac{1+x}{1-x}, \tag{4.1a}$$

$$x = \frac{y-M}{y+M}. \tag{4.1b}$$

The mapping can be utilized to construct an approximation on the finite interval. The method proposed by Boyd [2] has often been employed for the single domain problem. While the method has been used for the single domain case, we propose to extend its use to the multidomain approach. The idea is to use standard spectral elements in an area of the domain in which the solution might experience relatively rapid changes. Far away from this area, where the approximation does not experience such change, a semi-infinite domain is employed.

For example, given a simple 1D Helmholtz equation,

$$\begin{aligned} u_{xx} + \lambda u &= f, \\ x &\in (-\infty, \infty), \\ \lim_{x\to\infty} u(\pm x) &= 0, \end{aligned} \tag{4.2}$$

the area around the origin can be approximated using spectral elements with a finite subdomain. Away from the origin, semi-infinite subdomains can be employed. For the semi-infinite subdomains, the following functions are defined (the notation introduced by Boyd [2] is employed here),

$$\begin{aligned} LM_n(y) &= L_n\left(\frac{y-M}{y+M}\right) \\ &= L_n(x), \end{aligned} \tag{4.3}$$

where $L_n(x)$ is the n^{th} Legendre polynomial. To take advantage of the orthogonality of the Legendre polynomials, a weight function is required,

$$\begin{aligned} \int_0^\infty LM_n(y)LM_m(y)\frac{2}{(y+M)^2}dy &= \int_{-1}^1 L_n(x)L_m(x)dx \\ &= \frac{2}{2n+1}\delta_{nm}. \end{aligned} \tag{4.4}$$

Choosing the test function in the same manner as in section 2,

$$\phi M_j(y) = \begin{cases} \frac{1+x}{2} & j=0 \\ \frac{1-x}{2} & j=1 \\ L_j(x) - L_{j-2}(x) & j>1, \end{cases} \tag{4.5}$$

leads to a mass matrix that is identical to that used for the finite subdomains. The stiffness matrix is not as elegant as that found in section 2, though. The stiffness matrix, while not diagonal, is a banded matrix, with band width 5. While the new stiffness matrix is not symmetric, the new approximation can be employed for a much wider collection of boundary

conditions at infinity. In fact, the boundaries are enforced in exactly the same way as is done for a finite domain.

The stiffness matrix for the infinite subdomain is found in the same manner as for the finite subdomains,

$$\begin{aligned}(\mathcal{S}_N)_{mj} &= -\int_0^\infty \frac{d}{dy}\left(\phi M_j(y)\right)\frac{d}{dy}\left(\phi M_m(y)\frac{2M^2}{(y+M)^2}\right)dy \quad (4.6)\\ &= -\frac{M}{2}\int_{-1}^{1}\phi_j'(x)\frac{(1-x)^2}{2M}\phi_m'(x)\frac{(1-x)^2}{2M}dx\\ &\quad +\frac{M}{2}\int_{-1}^{1}\phi_j'(x)\phi_m(x)\frac{(1-x)^3}{2M^2}dx.\end{aligned}$$

The factor M should scale linearly to capture large scale variations in the solution [2]. However, because the method is defined to be used in conjunction with a spectral element method, an infinite domain can be "moved" further away from the origin by increasing the number of finite subdomains that are employed. One flexibility in the spectral element method is that it allows for greater resolution by increasing the number of subdomains.

4.2 Comparison with Laguerre polynomials

To employ this approach with the spectral element method, the basis functions are defined in exactly the same way. The basis functions, as defined, can be easily divided into those test functions that are zero on the subdomain boundaries, and those that are not zero on the subdomain boundaries. In this way the test functions that span two adjacent subdomains are defined in exactly the same way, and the implementation is a simple extension to the semi-infinite interval.

For example, to approximate equation (4.2), the domain is divided into non-overlapping subdomains. The interval $[-5,5]$ is divided into finite subdomains, the remaining two subdomains are $(-\infty,5]$ and $[5,\infty)$. Within each of the semi-infinite domains, an approximation is constructed from a linear combination of the basis functions defined in equation (4.5). The interval $[-5,5]$ is divided into four subdomains, the interval $(-\infty,5]$ is denoted subdomain 0, the interval $[5,\infty)$ is denoted subdomain 6, and the remaining subdomains, 1 through 4, are found from equally spaced finite intervals within $[-5,5]$. In this situation, the basis functions on subdomain n, $\phi_i^n(x)$, only have support on subdomain n for $i = 2\ldots N$. The functions $\phi_0^n(x)$ and $\phi_1^n(x)$ are used to construct basis functions whose support only includes adjacent subdomains and to enforce the boundary conditions.

To compare Laguerre polynomials and Boyd's mapping method, two separate situations are examined. The first is a situation where the solution decays to zero exponentially, and the second is a situation where

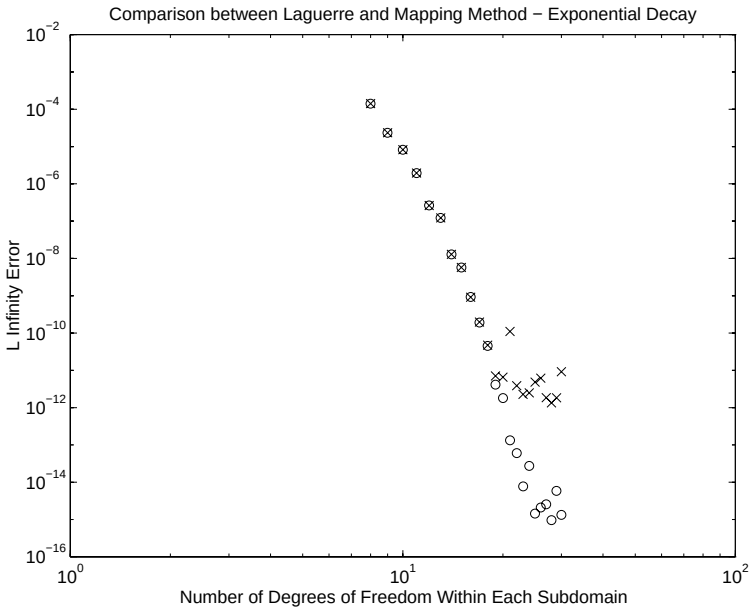

Figure 7: Spectral element approximation of a solution with exponential decay using Laguerre polynomials and algebraic mappings on the outer subdomains. The errors for the Laguerre polynomials are denoted by $\times$, while the errors for the mapping to the finite interval are denoted by $\circ$.

the solution decays to zero algebraically. In both of these examples, a 1D Helmholtz equations is examined, equation (4.2), and in both cases $\lambda = 2$. In the first example, the forcing function, $f(x)$, is $(2+\lambda)e^{-x^2} + 4x^2e^{-x^2}$, and in the second example the forcing function is $\frac{8x^2}{(1+x^2)^3} - \frac{2}{(1+x^2)^2} + \frac{\lambda}{1+x^2}$.

The L^∞ errors for the two trials are shown in Figures 7 and 10 (a brief discussion of the L^2 errors is given in Appendix A). The approximation that utilizes Laguerre polynomials does exhibit fast convergence to the equation whose solution decays to zero exponentially (Figure 7). However, this is not the case for the approximation to the equation whose solution does not decay as fast. The method using the proposed mapping, though, does exhibit similar convergence properties for both situations. Figures 9 and 10 demonstrate the L^∞ errors on the interval [-5,5] (the error is calculated only on the interval [-5,5]).

To test the method utilizing the mapping in a 2D case, a Poisson equa-

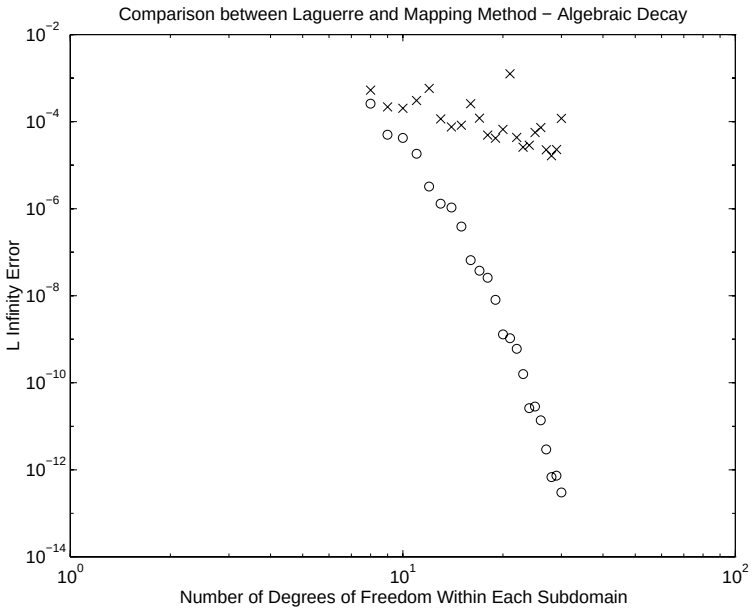

Figure 8: Spectral element approximation of a solution with algebraic decay using Laguerre polynomials and algebraic mappings on the outer subdomains. The errors for the Laguerre polynomials are denoted by $\times$, while the errors for the mapping to the finite interval are denoted by $\circ$.

tion is examined,

$$\begin{aligned} \triangle u &= \frac{4x^2+4y^2-4}{\left(1+x^2+y^2\right)^3}, \\ \lim_{x\to\infty} u(\pm x, y) &= 0, \\ \lim_{y\to\infty} u(x, \pm y) &= 0. \end{aligned} \tag{4.7}$$

The solution to this equation, $\frac{1}{1+x^2+y^2}$, decays to zero algebraically. In this test case 16 subdomains are employed. Four finite subdomains are employed on the unit square, $[-1,1]\times[-1,1]$. Away from the unit square semi-infinite subdomains are employed to construct an approximation (see Figure 11). The errors are shown in Table 1, and the errors are the maximum errors found on the abscissa of the Legendre-Gauss quadrature on each subdomain.

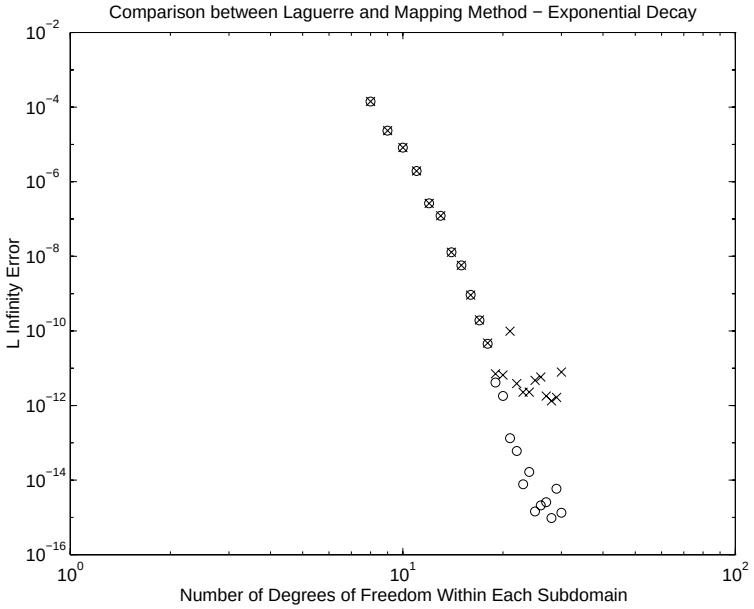

Figure 9: Spectral element approximation of a solution with exponential decay using Laguerre polynomials and algebraic mappings on the outer subdomains. The errors for the Laguerre polynomials are denoted by $\times$, while the errors for the mapping to the finite interval are denoted by $\circ$. The errors given are found by examining only the interval [-5,5].

$N_x = N_y$	L^∞ Error
8	5.206259e-04
10	2.438615e-04
12	1.365491e-04
14	7.567740e-05
16	4.658750e-05

Table 1: Maximum Errors for the approximation of a Poisson equation on an infinite domain. For each approximation 16 subdomains are employed, and the polynomial degree is given for each trial. For each trial the polynomial degree for both the x and y direction are equal.

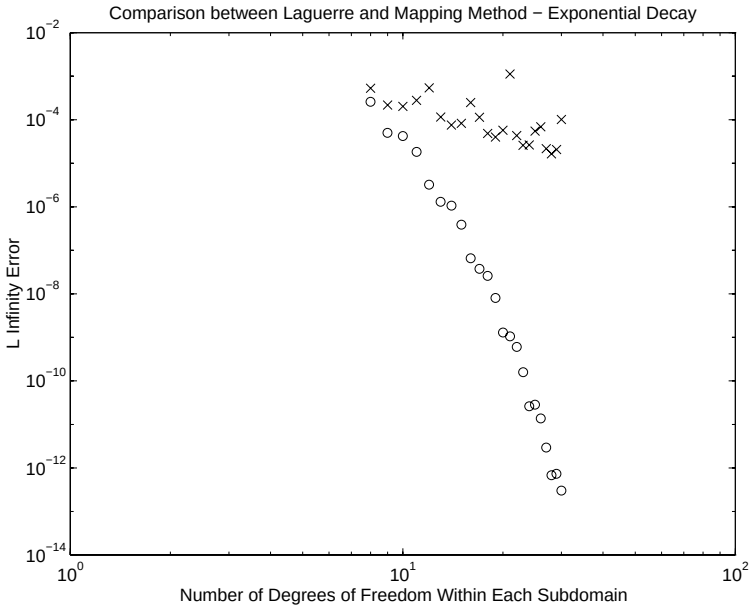

Figure 10: Spectral element approximation of a solution with algebraic decay using Laguerre polynomials and algebraic mappings on the outer subdomains. The errors for the Laguerre polynomials are denoted by $\times$, while the errors for the mapping to the finite interval are denoted by $\circ$. The errors given are found by examining only the interval [-5,5].

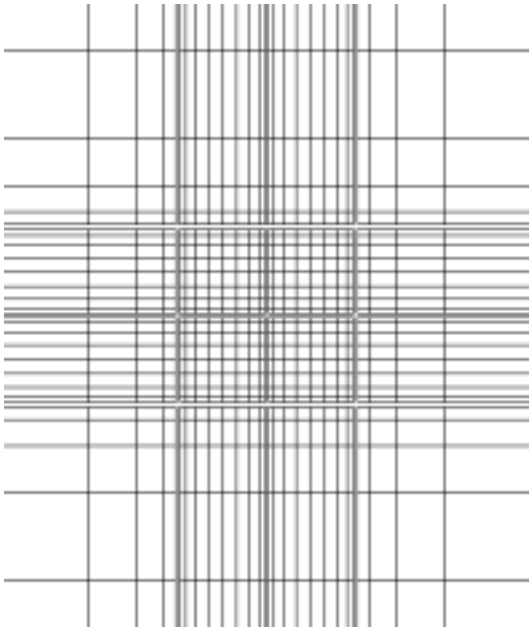

Figure 11: Close-up view of the domain decomposition for the 2D infinite domain. The grid is found from the abscissa of the Legendre-Gauss quadrature. The four finite subdomains are employed to decompose the unit square $[-1,1] \times [-1,1]$

A L^2 Errors for a Single Domain Approximation with Laguerre Polynomials

Theory for the convergence estimates of Laguerre polynomials are based on an L^2 norm [3, 11, 12]. In particular, the basis functions defined in section 3 are defined through the use of the Laguerre polynomials,

$$\begin{aligned} \phi_0(x) &= L_0^{(0)}(x)e^{-\frac{x}{2}}, \\ \phi_i(x) &= (L_i^{(0)}(x) - L_{i-1}^{(0)}(x))e^{-\frac{x}{2}}, \qquad i > 0. \end{aligned} \tag{A.1}$$

When the factor $e^{-\frac{x}{2}}$ is included in the basis functions, the relevant norm is the $L^2[0,\infty)$ norm [12].

$$||u|| = \int_0^\infty u^2(x)dx. \tag{A.2}$$

The integral can be approximated through the use of the Gauss quadrature.

As discussed by Boyd [2], the convergence of an approximation constructed through the use of Laguerre polynomials depends on the behavior of the solution at infinity. As a demonstration, a simple single domain approximation is examined. Approximations for two equations are examined,

$$\begin{aligned} u'' &= e^{-x}, \\ u(0) &= 1, \\ \lim_{x\to\infty} u(x) &= 0, \end{aligned} \tag{A.3}$$

and

$$\begin{aligned} u'' &= -2(1+x^2)^{-2} + 8x^2(1+x^2)^{-3}, \\ u(0) &= 1, \\ \lim_{x\to\infty} u(x) &= 0. \end{aligned} \tag{A.4}$$

The solution to equation (A.3), e^{-x}, decays to zero exponentially while the solution to equation (A.4), $\frac{1}{1+x^2}$, decays only algebraically.

The L^2 errors for both approximations is given in Figure 12. The results are similar to those when the L^∞ error are examined. The errors for the approximation to equation (A.3) demonstrate spectral convergence, while the approximation to equation (A.4) do not.

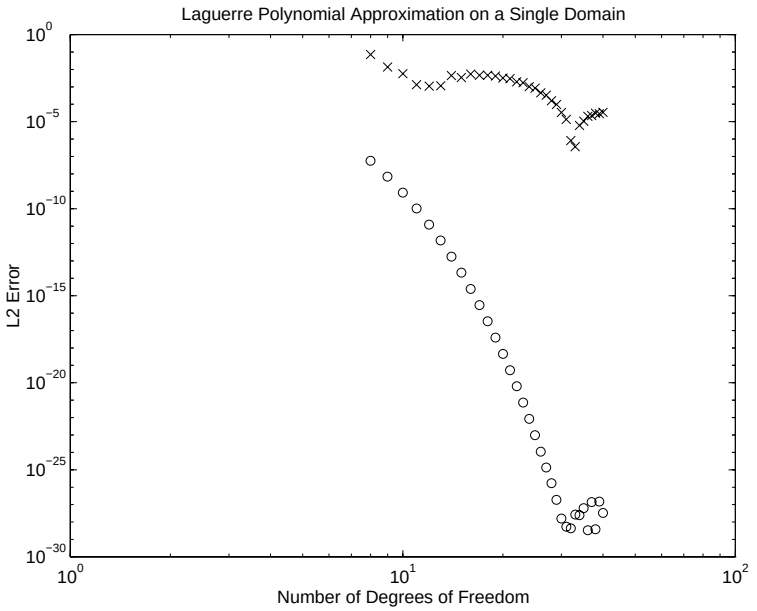

Figure 12: L^2 errors for a single domain approximation utilizing Laguerre polynomials. Errors for the approximation of a solution that decays to zero exponentially are denoted by an $\circ$ while errors for the approximation of a solution that decays only algebraically are denoted by an $\times$.

References

[1] P.M. Bellan. Alfen 'Resonance' Reconsidered: Exact equations for wave propagation across a cold inhomogeneous plasma, *Physics of Plasmas*, **1** (1994), 3523–3541.

[2] John Boyd. Orthogonal Rational Functions on a Semi-Infinite Interval, *Journal of Computational Physics*, **70** (1987), 63–68.

[3] O. Coulaud, D. Funaro, and O. Kavian. Laguerre spectral approximations of elliptic problems in exterior domains, *Computer Methods in Applied Mechanics and Engineering*, **80** (1990), 451–458.

[4] D. Funaro. Computational Aspects of Pseudospectral Laguerre Approximations, Tech. Report NAS1-18605, ICASE, NASA Langley Research Center, Hampton VA 23665-5225, October 1989.

[5] D. Funaro. *Polynomial Approximation of Differential Equations*. Berlin: Springer-Verlag, 1992.

[6] Philip M. Gresho and Robert L. Sani. On pressure boundary conditions for the incompressible Navier-Stokes equations, *International Journal for Numerical Methods in Fluids*, **7** (1987), 1111–1145.

[7] Walter Hauser. *Introduction to the Principles of Electromagnetism*. Reading, MA: Addison-Wesley, 1971.

[8] G. Karniadakis, M. Israeli, and S. Orszag. High-order splitting methods for the incompressible Navier-Stokes equations, *Journal of Computational Physics*, **97** (1991), 414–443.

[9] L.D. Landau and E.M. Lifshitz. *Electrodynamics of Continuous Media*, vol. 8 of Course of Theoretical Physics. New York: Pergamon Press, 1960.

[10] Y. Maday, A. Patera, and E. Rønquist. An operator-integration-factor splitting method for time-dependent problems: Application to incompressible flow, *Journal of Scientific Computing*, **5** (1990), 263–292.

[11] Y. Maday, B. Pernaud-Thomas, and H. Vandeven. Reappraisal of Laguerre Type Spectral Methods, *La Recherche Aerospatial* (English Addition), **6** (1985), 13–35.

[12] C. Mavriplis. Laguerre Polynomials for Infinite-Domain Spectral Elements, *Journal of Computational Physics*, **80** (1989), 480–488.

[13] Paolo Secchi. Well-Posedness for a mixed problem for the equations of ideal Magneto-Hydrodynamics, *Archivel der Mathematik*, **64** (1995), 237–245.

[14] J. Shen. Efficient spectral-Galerkin method I. Direct solvers of second and fourth-order equations using Legendre polynomials, *SIAM Journal of Scientific Computing*, **15** (1994), 1489–1505.

[15] S.K. Wilson. The effect of a uniform magnetic field on the onset of Marangoni convection in a layer of conducting fluid, *Quarterly Journal of Mechanics and Applied Mathematics*, **46** (1993), 211–248.

[16] S.K. Wilson. The effect of a uniform magnetic field on the onset of steady Marangoni convection in a layer of conducting fluid with a prescribed heat flux on its lower boundary, *Physics of Fluids*, **6** (1994), 3591–3600.

Department of Mathematics, University of New Hampshire, Durham, New Hampshire 03824

Communicated by John Lund